Excision of the endothelial blood–brain barrier insulin receptor does not alter spatial cognition in mice fed either a chow or high-fat diet

Joanne M. Gladding [1,*], Neda Rafiei, Caitlin S. Mitchell, Denovan P. Begg

School of Psychology, Faculty of Science, University of New South Wales, Australia

A B S T R A C T

Insulin is transported across the blood–brain barrier (BBB) endothelium to regulate aspects of metabolism and cognition. Brain insulin resistance often results from high-fat diet (HFD) consumption and is thought to contribute to spatial cognition deficits. To target BBB insulin function, we used Cre-LoxP genetic excision of the insulin receptor (InsR) from endothelial cells in adult male mice. We hypothesized that this excision would impair spatial cognition, and that high-fat diet consumption would exacerbate these effects. Excision of the endothelial InsR did not impair performance in two spatial cognition tasks, the Y-Maze and Morris Water Maze, in tests held both before and after 14 weeks of access to high-fat (or chow control) diet. The HFD increased body weight gain and induced glucose intolerance but did not impair spatial cognition. Endothelial InsR excision tended to increase body weight and reduce sensitivity to peripheral insulin, but these metabolic effects were not associated with impairments to spatial cognition and did not interact with HFD exposure. Instead, all mice showed intact spatial cognitive performance regardless of whether they had been fed chow or a HFD, and whether the InsR had been excised or not. Overall, the results indicate that loss of the endothelial InsR does not impact spatial cognition, which is in line with pharmacological evidence that other mechanisms at the BBB facilitate insulin transport and allow it to exert its pro-cognitive effects.

1. Introduction

Palatable diet consumption and dietary induced obesity (DIO) are associated with impairments to spatial cognition and memory (Arnold et al., 2014; Gladding et al., 2018; Heyward et al., 2012; Tran & Westbrook, 2017; Valladolid-Acebes et al., 2011). Potential mechanisms underlying DIO-related cognitive impairments are insulin resistance and impaired endothelial function of the blood–brain barrier (BBB) which are sequelae of obesity (Buie et al., 2019; Clegg et al., 2011). Administration of insulin into the central nervous system (CNS) can improve hippocampal-dependent spatial cognitive function in rodents (Gladding et al., 2018; Haj-ali et al., 2009; McNay et al., 2010; Moosavi et al., 2006) and declarative memory and functional cognitive performance in humans (Benedict et al., 2004; Craft et al., 2012; Reger et al., 2008).

Rats develop peripheral insulin resistance following 8 weeks, and neuronal insulin resistance in the CNS following 12 weeks, of maintenance on a high fat diet (HFD; Pratchayasakul et al., 2011). DIO mice which show insulin resistance in their cortical tissue also show impaired performance on spatial memory tasks such as the T-Maze (Arnold et al.,

2014). This diet-induced insulin-resistance is associated with impaired neurovascular coupling that characterizes endothelial dysfunction (Kuboki et al., 2000; Williams et al., 2002). However, most of the evidence to date regarding insulin's function at the endothelium has been uncovered in the context of the peripheral vasculature (Kisanuki et al., 2001; Kondo et al., 2003; Vicent et al., 2003) which functions quite differently to the BBB vasculature. The BBB contains tight junction complexes to protect against the transport of macromolecules into the CNS. Yet, insulin must cross the BBB to exert its pro-cognitive effects.

For decades, it had been widely assumed that insulin is transported into the CNS via saturable InsR-mediated transport across the BBB (see Rhea & Banks, 2019 for review). This theory originated from modelling in dogs (Baura et al., 1993; Schwartz et al., 1991) and mice (Banks et al., 1997) which revealed insulin had comparable transport kinetics to other metabolic peptides known to cross the BBB. In support of this early modelling, the transport of insulin between cerebrospinal fluid (CSF) and blood plasma appears to be restricted in healthy rats (Meijer et al., 2016) and even further so in people with obesity and insulin resistance (Kern et al., 2006). Yet, whether BBB insulin transport selectively or

specifically relied on the InsR remained unclear until very recently.

Recent evidence indicates that the endothelial InsR at the BBB is not essential for the primary transcytosis of insulin across the BBB into the brain. In a transgenic mouse model where the InsR was excised from BBB endothelial cells, loss of the InsR did not abolish insulin peptide transport, but it delayed the onset of downstream signalling (Konishi et al., 2017), which was accompanied by increased food intake and weight gain. Pairing this genetic manipulation with a HFD accelerated the development of systemic insulin resistance (Konishi et al., 2017), indicating both peripheral and central effects of excising the InsR in a DIO model (Konishi et al., 2017). Using the same transgenic model, radioactive insulin transport was measured to investigate insulin transcytosis across the BBB (Rhea, Rask-Madsen, et al., 2018), revealing that InsR binding but not total insulin transport was reduced in animals lacking the endothelial InsR (Rhea, Rask-Madsen, et al., 2018). Similarly, separate studies found that the application of an InsR inhibitor (S961) to cultured brain endothelial cells reduced downstream insulin signalling but not insulin peptide uptake (Gray et al., 2017). Notably, S961 application can reduce InsR binding without affecting peptide transport over time (Hersom et al., 2018). Together, these findings indicate that the BBB endothelial InsR regulates signalling related activities but is not necessary for transcytosis of insulin into the brain. In addition to *in vitro* models (Gray et al., 2017; Hersom et al., 2018), which allow for the study of insulin transcytosis in controlled conditions, *in vivo* models allow for functional characteristics of the BBB, such as unique junctional tightness, to be characterized (Konishi et al., 2017; Rhea, Rask-Madsen, et al., 2018). However, the functional effects of InsR excision or inhibition on cognition and behaviour are yet to be elucidated.

Therefore, the present study aimed to assess whether 1) genetic excision of the InsR from the BBB is sufficient to induce deficits to spatial cognition, and 2) whether such changes would be exacerbated by HFD treatment. We used a transgenic mouse model where InsRs were specifically excised from endothelial cells. First, brain microvessels were isolated to assess vascular structure and confirm excision of the InsR. Transgenic mice were then tested on the Morris Water Maze (MWM) and Y-Maze (YM) to assess differences in baseline spatial cognitive functioning. Following this initial assessment, mice were allocated to receive a HFD or chow diet for 16 weeks. During weeks 13–14, mice underwent the same battery of spatial cognitive tests to assess if the diet treatment exacerbated or induced any cognitive changes. In addition, during weeks 15–16, changes to peripheral metabolism were measured by insulin and glucose tolerance tests.

2. Materials and methods

2.1. Subjects

Subjects were 62 male transgenic InsR-flox Tie2-Cre mice bred at and obtained from Australian BioResources (Moss Vale, NSW) at 6 months of age. These mice were generated by crossing mice expressing Cre-recombinase under the endothelial-specific promoter/enhancer Tie2 with mice harboring loxP sites flanking exon 4 of the InsR gene, as described by Vicent et al. (2003). Briefly, animals heterozygous for the InsR loxP sites or missing the Tie2-Cre transgene represented phenotypically wildtype control animals (WT; Tie2$^{Cre +/+}$-InsR$^{+/-}$; Tie2$^{Cre -/-}$-InsR$^{+/+}$). When an animal contained both the Tie2-Cre transgene and homozygous InsR loxP (InsR-flox) alleles, the InsR was excised from endothelial cells, leading to a knockout animal (KO; Tie2$^{Cre +/+}$-InsR$^{+/+}$). These KO mice were used as a model of InsR resistance at the level of the BBB. To facilitate accurate food intake monitoring, mice were single housed in cages located in a climate-controlled colony room maintained on a 12-hour light/dark cycle (lights on 0700). While social isolation can be stressful for mice, the anxiolytic effects are minimal when isolation is started later into adulthood, relative to adolescence, after ample socialisation has occurred (Benfato et al., 2022; Rivera-Irizarry et al., 2020). Upon arrival to the facility, cages were assigned to one of the four

groups. The first group factor was based on genotype (*WT* and *KO* groups). Next, mice were weighed and assigned to the diet condition in a counterbalanced fashion for equal variance across treatment groups. Half received a chow diet (*CHOW* groups) and half received a high fat diet (*HFD* groups) resulting in final group sizes of 15 (groups *WT CHOW* and *WT HFD*) or 16 (groups *KO CHOW* and *KO HFD*) each. All experimental procedures were approved by the Animal Care and Ethics Committee at the University of New South Wales (ACEC 19/65B) and were conducted during the light cycle. Upon arrival, mice were allowed one week of handling and acclimation before experimental protocols commenced.

2.2. Diet & timeline

Following the completion of baseline spatial cognitive testing (pre-diet testing), mice received *ad libitum* standard laboratory chow or HFD (Specialty Feeds, Western Australia, Australia). The chow contained 4.6 % fat w/w (12 % kilocalories from fat; overall energy density 14.2 MJ/kg). The HFD contained 21 % fat w/w (40 % kilocalories from fat; overall energy density 19.2 MJ/kg) which was composed from safflower oil (1.5 g/100 g) and clarified butter/ghee (19.5 g/100 g). Diets were based on the American Institute of Nutrition Guidelines (AIN93). Mice were maintained on their respective diets until time of sacrifice (total 16 weeks). Spatial cognition tests were repeated in weeks 13–14 (post-diet testing) and in weeks 15–16 peripheral metabolic measurements were collected. Body weight and food intake were measured three times per week across the study. The food intake data are presented and analysed per animal, as each mouse was single housed to enable accurate food intake measurements. Unfortunately, the intake data for 16 mice had to be removed (n = 4 of each group) due to technical difficulties with sensitive measurement equipment (BioDaq) which was attempted before mice were returned to their home cages and continued to have their food intake monitored manually.

2.3. Behavioural protocols

The behavioural protocols for spatial cognitive Y-Maze (Dember & Fowler, 1959; Spence & Lippitt, 1946) and Morris Water Maze (Morris, 1981) assays were based on previous methodology (Gladding et al., 2018) and are briefly described below. Behaviour was recorded via Microsoft LifeCam for analysis using EthoVision software (Noldus IT, Netherlands).

2.3.1. Y-maze

The Y-Maze consisted of three identical size arms (arm dimensions: L 35 cm × W 5 cm × H 10 cm) that converged at a center zone. The maze was filled with standard cage bedding. A unique black and white printed geometric visual cue (5 cm × 5 cm) was attached at the end of each arm. Arms were assigned as either the start, familiar, or novel arm, and these remained the same across groups. To assess spatial reference memory (Kraeuter et al., 2019), mice underwent a 10-minute familiarization trial where they were placed into the maze at the distal end of the start arm but had no access to the novel arm. Following a one-hour retention interval, mice were returned to the maze, at the distal end of the start arm, and provided free access to explore all three arms for a 5-minute test. Spatial reference memory was measured as the percentage of time spent in the now accessible novel arm compared to the start or familiar arms, during the test trial.

2.3.2. Morris Water Maze

A circular maze was filled with water (24 ± 2C) which was rendered opaque by addition of non-toxic tempera powder (Staples Australia Pty Ltd, Mascot, NSW). Distal cues (distinct black geometric shapes; 15 cm × 15 cm) were fixed to cardinal points around the maze to guide mice. The platform (10 cm) was always in the target southeast quadrant. On Day 1, a 10 cm tall red flagpole was placed in the center of a round

platform (10 cm diameter) raised 5 mm above the water level. Each mouse underwent two familiarization trials where they were released from the opposite quadrant and given 60 s to find the platform. They were gently guided onto the platform if 60 s elapsed without finding it, remained on the platform for 15 s, and were then removed, dried, and placed in their home cage for a 5-minute inter-trial interval. Over the following three consecutive days (Day 2 to Day 4), each mouse received four 60-second acquisition trials per day, starting from a unique start point. The platform was covered in white tape and submerged 5 mm below the surface. In trials where mice failed to locate the platform within the allocated time, they were gently guided to it. They remained on the platform for 15 s between trials before being picked up and placed back into the tank at the next start position, until the 4 trials were complete. On Day 5, a 60 s probe test was conducted to assess spatial reference memory, whereby the platform was removed from the maze. Spatial reference memory was measured as 1) the latency to first cross the previous platform location and 2) the percentage of time spent swimming in the target quadrant relative to the other quadrants during the probe test. Daily means were calculated for escape latency times of each mouse and experimental group over the five days.

2.4. Histology

2.4.1. Microvessel isolation

Prior to the diet experiment, a subset of behaviorally naïve transgenic mice were euthanised for PCR analysis to verify the transgenic model. The protocol was adapted from Lee et al. (2019). Briefly, batches of 3 animals (matching genotypes; brains were pooled together to increase microvessel yield; $n^{\text{WT pooled}} = 7$, $n^{\text{KO pooled}} = 5$) were euthanised by i.p. injection of sodium pentobarbital (60 mg/kg; Virbac, Milperra, NSW) and upon absence of pedal reflexes, were decapitated immediately with scissors. Brains were washed in M199 (Sigma-Aldrich, NSW) on ice before being rolled on blotting paper 2–3 times to remove the outer meninges and macrovessels. The brain stems, cerebellums, and hypothalamuses were grossly dissected while the brains were in phosphate buffered saline (PBS) on ice. The remaining cortices were homogenized in 7 mL of cold M199 (9 strokes in a Dounce homogenizer), poured into a 15 mL conical tube and centrifuged at 1000g for 10 min at 4 C. Supernatant was removed and resuspended in 12 mL of 20 % Dextran (70,000 mw; Sigma-Aldrich, NSW) in PBS before the next centrifugation at 4500g for 15 min at 4C. Supernatant was removed again to reveal a small red pellet of microvessels. These were resuspended in 100 µL of 1 % Bovine Serum Albumin (BSA)/M199, which was then passed through a Falcon 40 µm cell strainer (Corning, VIC) atop a 50 mL conical tube. The filter was inverted and washed once more with 6–8 mL of 1 % BSA/M199 atop a new 50 mL tube, collecting the final microvessel suspension. A small volume (50uL) was smeared onto a microscope slide to visually inspect for microvessels under a light microscope. After confirmation, the suspension was centrifuged at 1000g for 15 min at 4 C. This pelleted suspension was then used for immunofluorescence to assess the structural morphology of the microvessels, and real-time PCR was used to quantify InsR and endothelial cell gene expression.

2.4.2. Immunofluorescence

This protocol closely followed that outlined by Lee et al. (2019). After microvessel isolation, a 40 µm strainer containing the microvessel suspension was washed in 4 % PFA for 15 min before being washed with PBS. Microvessels were then collected and centrifuged at 2000g for 10 min at 4C. The pellet was aspirated and resuspended in 400 µL of BSA/PBS and a 50 µL drop was left to dry on a microscope slide. A hydrophobic barrier pen was used to draw a barrier around the dried sample, which was permeabilized with 0.1 % Tween/PBS for 15 min before blocking for 1 h with 5 % BSA/PBS. The sample was then incubated overnight with 1:200 anti-rabbit PECAM1/CD31 primary antibody (Sigma-Aldrich #SAB5700639; platelet endothelial cell adhesion molecule 1 or cluster of differentiation 31, an endothelial marker). The

following day, samples were lightly washed with 0.1 % Tween/PBS and incubated for 1 h with the secondary antibody AF647 (1:400). Following three more washes with 0.1 % Tween/PBS samples were counterstained with DAPI (1:1000) for 1 min before a final 0.1 % Tween/PBS wash. Slides were allowed to air dry before mounting and cover slipping with Vectashield mounting medium and imaging on a confocal microscope.

2.4.3. Real-time PCR

RNA was extracted from the final pelleted microvessel suspension (pooled from 3 brains) using Trireagent. RNA quality was determined via NanoDrop Lite (Thermofisher Scientific) and converted to cDNA (Life technologies, SuperScript III First-Strand Synthesis). Real-Time PCR was performed with gene specific TaqMan primers (Applied Biosystems; Table 1). Reactions were performed in triplicate with the following cycling protocol: 360 s heat start at 95 °C, 45 cycles of denaturation at 95 °C for 25 s, annealing at 59 °C for 30 s, and extension at 72 °C for 20 s. Fluorescence detection was performed at 72 °C. Relative expression was normalized to the geometric mean of housekeeping genes *ribosomal protein S18 (RPS18)* and *GAPDH*. Gene expression was calculated for the InsR and PECAM1/CD31, a transmembrane protein highly expressed in endothelial cell linings and commonly used for endothelial identification (Goncharov et al., 2017). Data are presented as the standardized change in expression levels as a fraction of the WT control levels. Inconclusive data were excluded (CT $> \sim 36$).

2.5. Peripheral metabolism

Following diet treatment and post-diet behavioural testing, insulin and glucose tolerance tests were conducted to assess peripheral sensitivity to insulin. Blood samples were taken from a tail tip cut after application of local anesthetic (2 % lidocaine gel). For the insulin tolerance test (ITT), mice were placed into clean cages and received an i. p. injection of insulin (0.2U/mL; 1U/kg body weight, diluted in saline). Blood glucose levels were sampled from the tail tip at 0, 15-, 30-, 45-, and 60-minutes post injection using a glucometer (Accuchek Performa). One week later, the glucose tolerance test (GTT) was conducted. After overnight fasting, mice were placed into clean cages, and blood was collected in capillary tubes (Microvette EDTA) from the tail tip prior to i. p. injection of glucose (0.2 mg/mL; 1 g/kg body weight, diluted in saline) and at 15 min post injection for insulin assay. Blood was sampled at 0, 15-, 30-, 60-, and 120-minutes post injection for glucose concentrations using a glucometer (Accuchek Performa). Blood samples collected from GTT tail cuts (maximum sample of 200 µL) were centrifuged at 12,000 rpm at 4 C for 10 min to separate plasma from red blood cells and platelets. The top plasma layer was aspirated into new storage tubes and kept at −80 C. Plasma insulin levels were later assessed via Ultra-Sensitive Mouse Insulin ELISAs (#90080, Crystal Chem, USA) as per the manufacturer instructions.

2.6. Statistical analysis

Data were analysed using planned orthogonal contrasts, testing for main effects of diet, genotype, time, maze location (arm, quadrant), and training day. This procedure has been described by Hays (1963) and all of the analyses were conducted using the PSY software (School of

Table 1
Assay IDs for TaqMan Gene expression analyses. Obtained from ThermoFisher Scientific.

Gene	Assay ID
RPS18	*Mm02601777_g1*
GAPDH	*Mm99999915_g1*
InsR	Mm01211875_m1
PECAM1	Mm00476712_m1

Psychology, The University of New South Wales, Australia). The Type I error rate was controlled at alpha = 0.05 for each contrast tested. If interactions were detected, follow-up simple effect analyses were conducted to determine the source of the interactions. Metabolic data were excluded for an animal if any blood glucose readings were missed across the 60- and 120-minute tests (n = 5). Behavioural data were excluded if the camera failed to record an animal's trial correctly, the EthoVision software could not detect the animal appropriately, or, in the case of the Y-Maze, an animal climbed into the novel arm during the familiarization trial (n = 5). Final group numbers are listed in the figure legends accordingly.

3. Results

3.1. Validation of the transgenic model: excision of the InsR from endothelial cells

Prior to commencing the diet protocol, the primary aim was to validate an effective excision of the InsR at the endothelial membrane of brain microvessels in KO mice. To do so, microvessels were isolated from behaviorally naïve mice. Fresh brains were excised, and morphology was assessed by light microscopy and immunofluorescence staining for endothelial marker CD31 and DAPI (Fig. 1A-B). Following this, mRNA expression of the endothelial marker PECAM1/CD31 and the InsR were analysed using real-time PCR. The data are presented in Fig. 1C as the fraction change in expression of these proteins in the KO relative to WT mice. PECAM1 expression did not significantly differ between WT and KO mice (Genotype: $F_{(1,7)} = 0.126$, p = 0.73), indicating all vessels were intact. The excision of the InsR was successful, as there tended to be lower InsR mRNA expression in the KO mice (Genotype: $F_{(1,7)} = 4.14$, p = 0.08). Additional microvessel extractions were planned to confirm this statistical trend but were not completed due to Covid-19 laboratory restrictions and subsequent laboratory power outages during extractions which resulted in a substantial loss of samples. To avoid the unnecessary euthanasia of further mice, given that we saw a 50 % arithmetic decrease in InsR mRNA and that the validity of the model in excising the InsR from the endothelium has been demonstrated before (Roudnicky et al., 2017; Vicent et al., 2003), the diet experiment was commenced.

### 3.2. Food intake, body weight, and metabolic parameters

3.2.1. Food intake and body weight

Body weight and food intake across the 16-week protocol are presented in Fig. 2. Mice either received a chow diet (groups *WT CHOW* and *KO CHOW*) or a HFD (groups *WT HFD* and *KO HFD*). Food intake data are presented over the first 14 weeks only, because food was intermittently removed overnight during the GTT, making the data for the final two weeks incomplete. At the beginning of the diet period (week 1, Fig. 2B), CHOW and HFD groups did not differ in body weight (Diet: $F_{(1,58)} = 0.02$, p = 0.89). However, KO groups weighed 5 % more than WT groups (Genotype: $F_{(1,58)} = 4.36$, p = 0.04; mean ^{WT} 30.81 g ± 0.56; mean ^{KO} 32.51 g ± 0.57). Over the course of the diet protocol, the HFD groups consumed more calories than the CHOW groups (Diet: $F_{(1,42)} = 42.40$, p < 0.001; Fig. 2A). The number of calories consumed gradually decreased over time (Week: $F_{(1,42)} = 28.26$, p < 0.001), with a greater decrease in the HFD groups (Diet × Week: $F_{(1,42)} = 5.60$, p = 0.02). The caloric intake also depended on genotype (Week × Genotype interaction: $F_{(1,42)} = 9.22$, p < 0.01). Simple effects revealed that while CHOW intake decreased slightly over time (Week: $F_{(1,21)} = 4.45$, p = 0.047), this only approached significance in the KO CHOW group (Genotype × Week: $F_{(1,21)} = 3.57$, p = 0.07) whereas the WT CHOW group had stable intake. HFD intake also decreased over time (Week: $F_{(1,21)} = 28.82$, p < 0.001) and this decrease was greater in the KO HFD than WT HFD group (Genotype × Week interaction: $F_{(1,21)} = 5.76$, p = 0.026). While KO groups may have shown larger changes in food intake over time, overall energy intake did not differ from WT groups (Genotype: $F_{(1,42)} = 0.01$, p = 0.92). During the diet protocol, there was a steady increase in body weights (Week: $F_{(1,58)} = 458.41$, p < 0.001), with greater weight gain in HFD groups (Diet: $F_{(1,58)} = 84.44$, p < 0.001) and at a faster rate (Diet × Week interaction: $F_{(1,58)} = 136.77$, p < 0.001) than CHOW groups. KO groups tended to weigh more than WT groups over the course of the diet protocol (Genotype: $F_{(1,58)} = 3.64$, p = 0.06), but this was not diet-dependent (Genotype × Diet: $F_{(1,58)} = 0.04$, p = 0.84).

3.2.2. Insulin tolerance test

The weight gain and DIO of the HFD groups was associated with peripheral insulin insensitivity on the ITT (Fig. 2C-D). After a peripheral injection of insulin all mice were responsive to insulin, with each blood glucose reading lower than the previous time point (Time: $F_{(1,53)} = 884.99$, p < 0.001; Fig. 2C). Blood glucose levels tended to fall more slowly in the KO groups relative to WT groups over time (Genotype × Time: $F_{(1,53)} = 3.70$, p = 0.06), but over the entire hour glucose readings were equivalent (Genotype: $F_{(1,53)} = 0.20$, p = 0.66). While the change in blood glucose over time did not differ between diet groups (Diet × Time: $F_{(1,53)} = 0.68$, p = 0.41), blood glucose levels were elevated in HFD relative to CHOW groups at every time point across the one-hour ITT (Diet: $F_{(1,53)} = 9.70$, p < 0.01), demonstrating their reduced sensitivity to insulin. This was corroborated by an area under
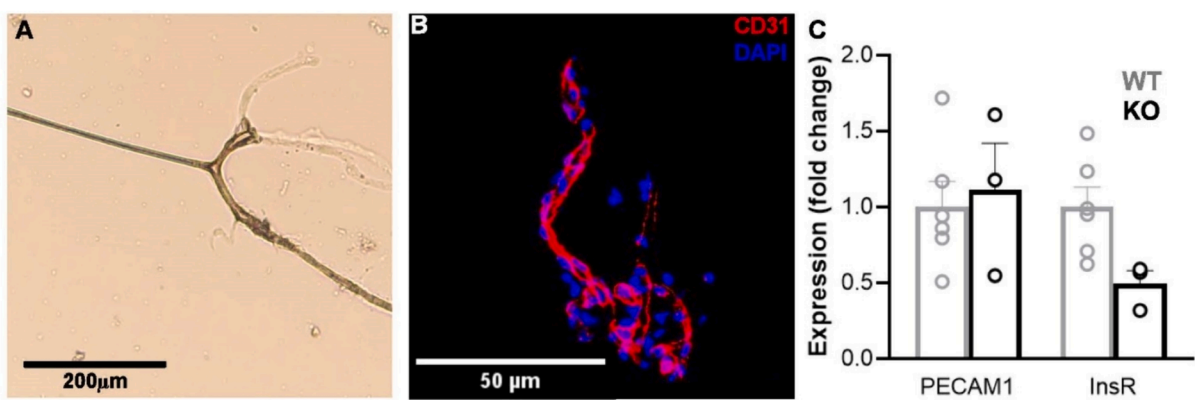
Fig. 1. Isolated microvessels. *A) Light microscope image of intact isolated microvessel. B) Confocal microscope image showing continuous stain of brain endothelial cells, CD31 (red) in the microvessel, counterstained with nuclear stain DAPI. C) InsR expression tended to be lower in KO mice relative to WT mice, and PECAM1 endothelial expression was equivalent between the groups. Data are presented as the fold change relative to housekeeping genes RPS18 and GAPDH ± SEM. Final $n^{WT\ pooled} = 6$, $n^{KO\ pooled} = 3$..*
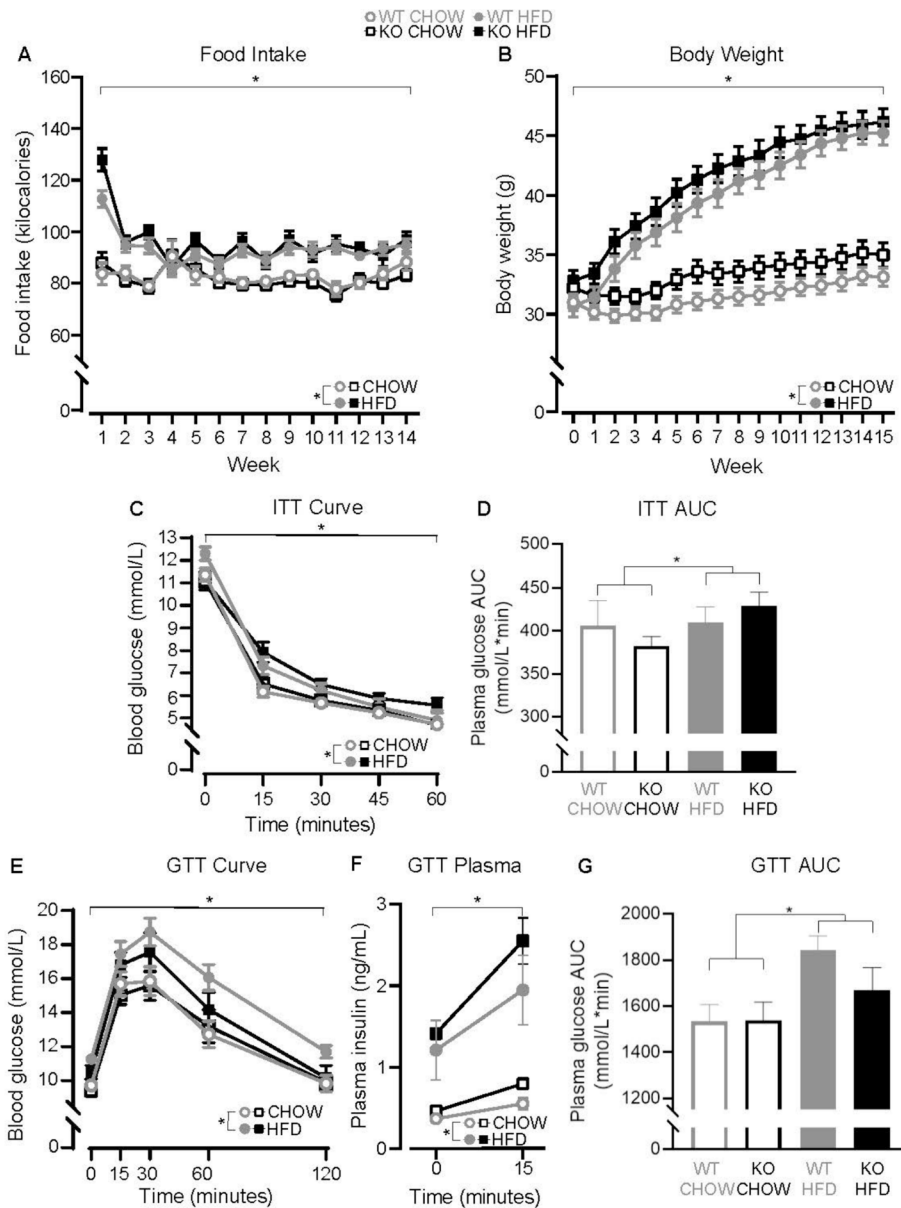
Fig. 2. HFD mice consumed more calories, gained more weight, and were peripherally insensitive to insulin and glucose relative to WT mice. A) *Food intake data are presented as mean kilocalories consumed per mouse, per week. Over time food intake decreased, and this effect was significantly larger in HFD mice.* $n^{WT\ groups} = 11$ *each;* $n^{KO\ groups} = 12$ *each.* **B)** *Body weight data are presented as body weight (grams). HFD mice consumed more calories and gained significantly more weight compared to CHOW mice. KO groups tended to weigh more than WT groups.* $n^{WT\ groups} = 15$ *each;* $n^{KO\ groups} = 16$ *each.* **C)** *HFD caused insulin insensitivity with a significantly smaller reduction in blood glucose after insulin injection. Insulin insensitivity tended to be exacerbated in KO mice.* **D)** *Area under the curve (AUC) analysis showing higher blood glucose levels in HFD groups across the ITT.* **E)** *HFD produced glucose intolerance with significantly greater blood glucose levels after glucose injection.* **F)** *HFD mice displayed significantly higher basal blood insulin levels which remained after glucose injection.* **G)** *AUC analysis showing higher blood glucose levels in HFD groups during GTT. Panels C-G,* $n^{WT\ CHOW} = 13\text{-}15$, $n^{WT\ HFD} = 14\text{-}15$, $n^{KO\ CHOW} = 15\text{-}16$, $n^{KO\ HFD} = 15\text{-}16$. *Data are shown as mean ± SEM.* * = p < 0.05 *for main effects of Week (A & B), Time (C, E, & F), and Diet (all panels) as indicated on each panel.*

the curve (AUC; Fig. 2D) analysis which similarly showed no difference between WT and KO groups (Genotype: $F_{(1,53)} = 0.87$, p = 0.35) but significantly greater AUC in HFD compared to CHOW groups (Diet: $F_{(1,53)} = 8.44$, p < 0.01). There was no exacerbation of HFD-induced insulin insensitivity in KO mice as indicated by blood glucose levels (Diet × Genotype: $F_{(1,53)} = 0.05$, p = 0.83) or AUC (Diet × Genotype: $F_{(1,53)} = 0.24$, p = 0.63).

3.2.3. Glucose tolerance test

The data demonstrate that 15 weeks of HFD treatment resulted in glucose intolerance on an intraperitoneal GTT (Fig. 2E-G). After a peripheral injection of glucose, blood glucose increased over time (Time: F

$(1,58) = 6.70$, p < 0.05; Fig. 2E), with HFD groups exhibiting elevated blood glucose levels relative to CHOW groups at every time point (Diet: $F_{(1,58)} = 9.35$, p < 0.01), indicating reduced clearance of glucose. There were no main or interaction effects involving genotype (Genotype: $F_{(1,58)} = 0.25$, p = 0.25; Diet × Genotype: $F_{(1,58)} = 0.89$, p = 0.35; Genotype × Time: $F_{(1,58)} = 0.10$, p = 0.75; Fig. 2E). An AUC analysis (Fig. 2G) similarly showed no difference between WT and KO groups (Genotype: $F_{(1,58)} = 1.09$, p = 0.30) but significantly greater AUC in HFD compared to CHOW groups (Diet: $F_{(1,58)} = 7.58$, p < 0.01) which was not exacerbated in KO mice (Diet × Genotype: $F_{(1,58)} = 1.25$, p = 0.27). Plasma insulin levels were elevated in HFD groups at baseline (0 min) and 15 min post-glucose (Diet: $F_{(1,53)} = 36.15$, p <

0.001; Fig. 2F). While circulating insulin levels increased over the 15 min (Time: $F(1,53) = 47.40$, $p < 0.001$) this increase was greater in the HFD groups (Diet × Time: $F(1,53) = 15.19$, $p < 0.001$) and did not depend on genotype (Diet × Genotype: $F(1,53) = 0.32$, $p = 0.58$). Overall, these data show a greater level of basal circulating insulin and a larger release of insulin into the bloodstream to reduce blood glucose levels in the HFD groups.

3.3. Spatial cognition

3.3.1. Baseline/pre-diet

At baseline, there were no significant differences in behaviour between the future CHOW and HFD groups on the YM or MWM (Diet, Diet × Genotype; Fs < 3.78). The test trial of the YM (Fig. 3A) showed that all mice spent comparable time in the start and familiar arms (Genotype × Control Arms: $F(1,49) = 0.38$, $p = 0.54$) and more time overall in the novel arm (Arm: $F(1,49) = 20.28$, $p < 0.001$). Importantly, there were no differences in YM test performance between WT and KO groups (Genotype: $F(1,49) = 0.03$, $p = 0.86$; Genotype × Novel Arm: $F(1,49) =$

0.01, $p = 0.92$) indicating that spatial cognition was intact in WT and KO mice (Fig. 3A). During MWM training (Fig. 3B), there were no significant group differences in time taken to find the visible platform on the first training day (Genotype × Visible Day: $F(1,58) = 0.21$, $p = 0.65$). Escape latencies decreased over the three hidden training days (Hidden Day: $F(1,58) = 88.17$, $p < 0.001$) regardless of group (Genotype × Hidden Day: $F(1,58) = 0.01$, $p = 0.92$). Mice spent the least time in the furthest quadrant and the most time in the target quadrant (Fig. 3C; Quadrant: $F(1,58) = 62.15$, $p < 0.001$), and this did not differ between groups (Genotype × Quadrant: $F(1,58) = 2.38$, $p = 0.13$; Fig. 3C). Likewise, on test day there were no differences in latency to reach the previous platform location (Genotype × Test Day: $F(1,58) = 0.04$, $p = 0.84$). Altogether, the InsR excision from endothelial cells did not induce a spatial cognitive deficit on the YM or MWM.

3.3.2. Post-diet

After 12 weeks on the diet protocol, mice underwent a second round of spatial-cognitive tests (YM and MWM), to assess HFD-induced cognitive deficits and whether these were exacerbated by the excision
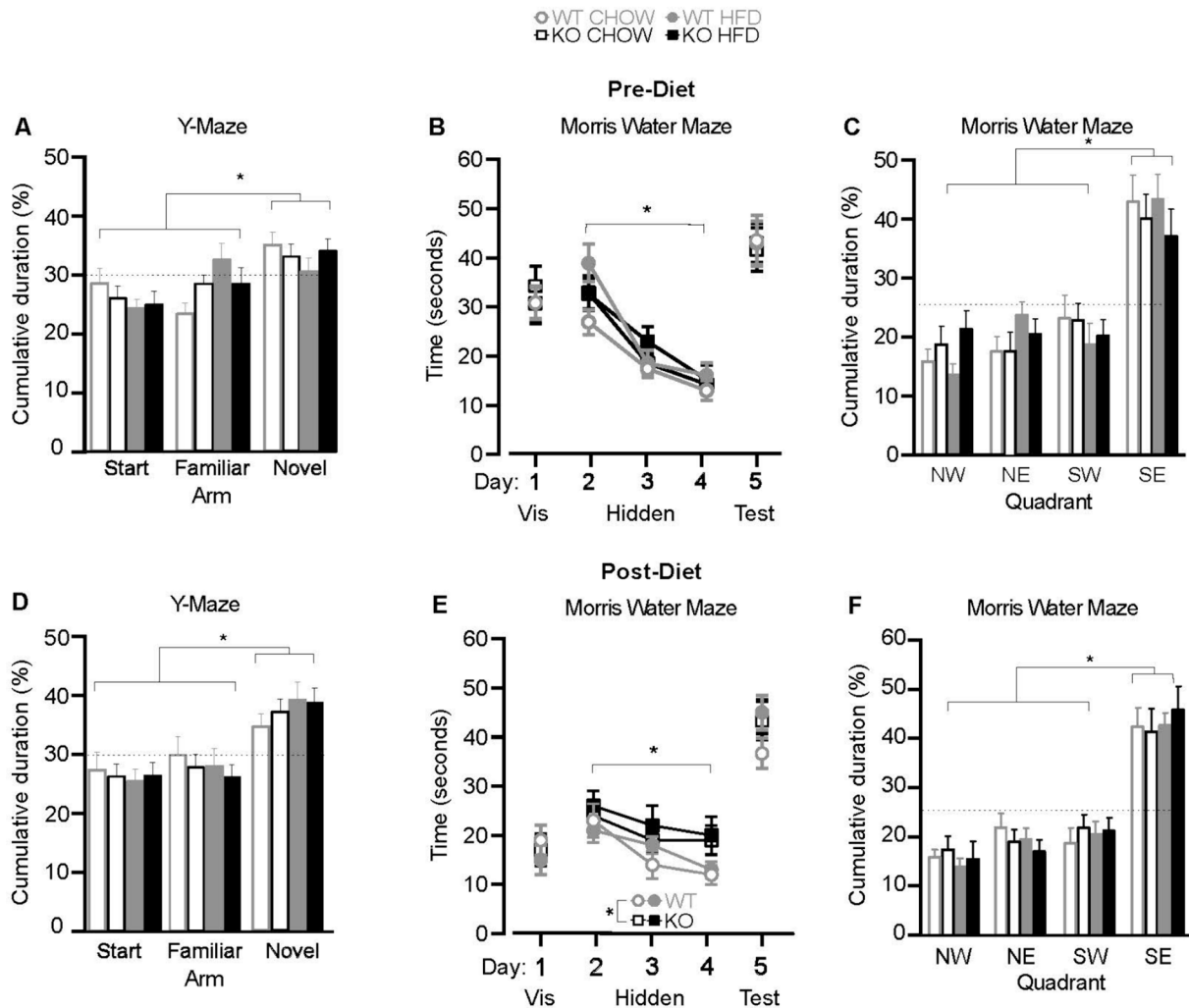
Fig. 3. **Pre-diet and post-diet spatial memory on the Y-Maze and Morris Water Maze was intact in all groups.** *A & D) All mice spent significantly more time in the novel arm of the YM versus the start and familiar arms pre- and post-diet. B & E) Mean escape latencies of the MWM did not differ on the visible (Vis) platform training day. All groups reached the platform faster across the hidden platform days pre- and post-diet. Post-diet, KO mice were significantly slower than WT mice to find the platform during hidden platform days. All mice took the same amount of time to reach the previous platform location on the test day pre- and post-diet. C & F) All mice spent significantly more time in the target SE quadrant than the other quadrants pre- and post-diet. Dotted lines represent chance level. Data are shown as mean ± SEM. * = p < 0.05 for main effects of Arm (A & D), Day (B & E), Quadrant (C & F), and Genotype (E) as indicated on each panel. MWM: northwest (NW), northeast (NE), southwest (SW), southeast (SE). $n^{WT\ CHOW} = 15$, $n^{WT\ HFD} = 15$, $n^{KO\ CHOW} = 16$, $n^{KO\ HFD} = 16$. Y-Maze: pre-diet, $n^{WT\ CHOW} = 13$, $n^{WT\ HFD} = 14$, $n^{KO\ CHOW} = 12$, $n^{KO\ HFD} = 14$. Y-Maze: post-diet, $n^{WT\ CHOW} = 13$, $n^{WT\ HFD} = 15$, $n^{KO\ CHOW} = 14$, $n^{KO\ HFD} = 16$.*

of the InsR from endothelial cells. Data from the YM test trial is presented in Fig. 3D. All mice spent comparable time in the start and familiar arms (Genotype × Control Arms: $F_{(1,54)} = 0.05$, $p = 0.82$; Diet × Control Arms: $F_{(1,54)} = 0.25$, $p = 0.62$) and overall more time in the novel arm (Arm: $F_{(1,54)} = 35.65$, $p < 0.001$; Fig. 3D). Neither the HFD treatment (Diet × Novel Arm: $F_{(1,54)} = 0.34$, $p = 0.56$) nor InsR excision (Genotype × Novel Arm: $F_{(1,54)} = 1.61$, $p = 0.2$; Diet × Genotype × Novel Arm: $F_{(1,54)} = 0.36$, $p = 0.55$) induced a cognitive deficit, with all mice spending equivalent time in the novel arm. For the MWM (Fig. 3E), there were again no significant group differences in time taken to find the visible platform on the first training day (Visible Day × Genotype: $F_{(1,58)} = 0.03$, $p = 0.87$; Visible Day × Diet: $F_{(1,58)} = 0.31$, $p = 0.58$; Visible Day × Diet × Genotype: $F_{(1,58)} = 0.80$, $p = 0.38$). Over the three hidden training days, mice gradually reached the platform faster (Hidden Day: $F_{(1,58)} = 13.43$, $p < 0.001$), regardless of diet (Hidden Day × Diet: $F_{(1,58)} = 0.06$, $p = 0.80$) and genotype (Hidden Day × Diet: $F_{(1,58)} = 0.98$, $p = 0.33$). Overall though, KO groups were slower to reach the platform than WT groups (Genotype: $F_{(1,58)} = 4.49$, $p = 0.038$), but this was not influenced by the diet treatment (Diet: $F_{(1,58)} = 0.25$, $p = 0.62$; Diet × Genotype: $F_{(1,58)} = 0.05$, $p = 0.83$). On the test day, latency to reach the previous platform location did not differ between the groups. There was no spatial deficit in KO mice (Test Day × Genotype: $F_{(1,58)} = 1.25$, $p = 0.27$), and like the YM, the HFD did not induce a spatial memory impairment either (Test Day × Diet: $F_{(1,58)} = 0.40$, $p = 0.53$), regardless of whether the InsR was excised or not (Test Day × Diet × Genotype: $F_{(1,58)} = 2.79$, $p = 0.10$). All groups spent the most time in the target quadrant (Quadrant: $F_{(1,58)} = 85.34$, $p < 0.001$; Fig. 3F), further indicating they remembered the previous platform location. This was not altered by the diet treatment (Diet × Quadrant: $F_{(1,58)} = 0.46$, $p = 0.50$) or InsR excision (Diet × Genotype: $F_{(1,58)} = 0.02$, $p = 0.89$; Diet × Genotype × Quadrant: $F_{(1,58)} = 0.20$, $p = 0.66$). In summary, all groups demonstrated intact spatial memory by showing preference for the southeast quadrant during the probe test, and similar latencies to reach the previous platform location on Day 5. However, KO groups were slower to learn the location of the platform during training.

4. Discussion

This study tested whether genetic excision of the InsR from the BBB was sufficient to induce hippocampal-dependent spatial cognition deficits and whether any deficits would be exacerbated by HFD treatment. This was achieved by genetically excising the endothelial InsR from the BBB of adult male mice and placing them on a HFD for 16 weeks. Spatial cognition was tested on the YM and MWM pre- and post-diet. Notably, KO mice fed a chow diet weighed more than WT mice and demonstrated accelerated peripheral insulin insensitivity in a similar fashion to a previous transgenic *in vivo* endothelial InsR model (Konishi et al., 2017).

4.1. Effect of the InsR excision

Excision of the endothelial InsR was not sufficient to induce spatial cognitive deficits. Adult male KO mice did not demonstrate any impairments in pre-diet cognitive performance on the YM or MWM. Given that insulin can enhance cognition (Benedict et al., 2004; Gladding et al., 2018; Haj-ali et al., 2009; McNay et al., 2010; Moosavi et al., 2006), and that these mice lacked the InsR as a means of transport into the brain, this strongly suggests that insulin was still gaining access to the brain. Although we had no direct measure of insulin transport here, this is supported by pharmacokinetic evidence that the BBB InsR is involved in signalling but not transcytosis of insulin at the BBB (Hersom et al., 2018; Konishi et al., 2017; Rhea & Banks, 2019; Rhea, Rask-Madsen, et al., 2018). Thus, a novel transporter protein may exist at the BBB to permit insulin entry in order to leave spatial cognition intact. Since BBB endothelial cells create a barrier to other cells, it is not that surprising that these cells would contain a transporter protein to independently

move insulin to other cell types. The novel insulin transporter versus the signalling InsR could be regulated differently, and independently, by the physiological state (Rhea & Banks, 2019). Alternatively, the intact hippocampal-dependent cognition that we observed could be explained by the brain's capacity for *de novo* biosynthesis of insulin (see Dakic et al., 2023 for review). It has been demonstrated that hippocampal neuronal stem cells can produce insulin expressing cells and that subpopulations of neurons in the hippocampus produce *de novo* insulin, as indicated by the presence of C-peptide (commonly used to measure levels of insulin production) (Kuwabara et al., 2011). Whether insulin is biosynthesized by the brain in quantities that can support cognition and eliminate the requirement for peripheral insulin requires further investigation. The current consensus is that the primary source of brain insulin is peripheral, from the pancreas.

Loss of the endothelial InsR was sufficient to alter the weight and peripheral metabolism of KO mice. In line with a previous transgenic model of BBB InsR excision in male mice (Konishi et al., 2017), our male KO mice weighed more than WT mice at baseline before commencing the diet treatment. These mice also showed some indications of heightened insulin insensitivity on the insulin tolerance test. After an intraperitoneal injection of insulin, blood glucose levels tended to fall more slowly in KO relative to WT mice. This corroborates with the heightened insulin insensitivity demonstrated previously (Konishi et al., 2017). A loss of insulin sensitivity in KO mice was reported in the first 30 min after insulin injection, before glucose readings fell back in line with control mice (Konishi et al., 2017).

4.2. Effect of the diet treatment

Twelve weeks of HFD consumption and DIO left performance on both the YM and MWM intact. This was unexpected given prior evidence that HFD treatment induces hippocampal-dependent spatial cognition deficits (Arnold et al., 2014; Gladding et al., 2018; Heyward et al., 2012; Tran & Westbrook, 2017), notwithstanding the underreporting of null effects in preclinical literature (Foster & Putos, 2014). Nevertheless, others have reported a lack of cognitive deficits in mice on the YM and MWM after HFD treatment (Leyh et al., 2021), which was attributed to a combination of factors including age, task parameters, diet type, and lack of other risk factors. Age during HFD exposure (e.g., adolescence versus adulthood) has been shown to variably impact cognition, with adolescence being a particularly vulnerable period (Boitard et al., 2014; Boitard et al., 2012). Here, one possible explanation for the lack of diet-induced deficits is that the baseline pre-diet spatial training afforded some protection against HFD induced hippocampal changes. Indeed, a prior study has shown that pre-training on place recognition protected rats against DIO-induced impairments in a task-specific way (Tran & Westbrook, 2017). It is possible that pre-training preserves specific spatial rules, and that HFD feeding does not disrupt these rules or the ability to use and retrieve them (Tran & Westbrook, 2017). Pre-training on hippocampal-dependent tasks including the MWM and a context fear conditioning task is also sufficient to mitigate deficits induced by NMDA receptor antagonism (Bannerman et al., 1995; Sanders & Fanselow, 2003). Further, training on the MWM increases hippocampal InsR expression and signalling (Zhao et al., 1999), and insulin supports spatial memory performance (Gladding et al., 2018; McNay et al., 2010; Moosavi et al., 2006). As such, the baseline cognitive testing may have inadvertently induced metaplasticity, thus providing protection against or counteracting any subsequent diet-related changes to the hippocampus. Notably, the cognitive protection previously afforded by pre-training (Tran & Westbrook, 2017) occurred after relatively extensive pre-diet training (i.e., 3 training/test sessions) and our mice were similarly extensively trained on two hippocampal-dependent tasks over several days. Yet, another cohort of mice that are not pre-trained prior to HFD exposure would be needed to confirm this theory. From an ecological perspective, this would suggest that the effects of obesogenic diets on cognition might be restricted to newly acquired skills,

memories, or behaviours. Whether this extends to hippocampal-independent tasks, such as Pavlovian or instrumental conditioning, would be interesting to determine. Future studies are warranted to test the effects of obesogenic diets on new versus old memories and characterize the protective nature of pre-diet training.

4.3. Interactions between the InsR excision and diet treatment

Our results show that HFD treatment did not interact with the genetic excision of the InsR from endothelial cells to induce or exacerbate metabolic deficits. Regardless of diet, KO groups tended to weigh more than WT groups and tended to show a slower reduction in blood glucose in the insulin tolerance test. Genetic excision of the InsR at the BBB was previously associated with greater basal weight gain in male mice, relative to a wildtype control group, and this was also not accelerated by 4 months of HFD feeding (Konishi et al., 2017). However, unlike the previous transgenic model (Konishi et al., 2017), we did not observe an exacerbation of HFD-induced ITT insulin insensitivity or glucose intolerance in our KO HFD mice. These metabolic differences could be explained by the higher fat content of their diet (60 % vs. 40 % HFD) or differences in glucose delivery (oral vs. i.p.). Finally, our models were driven by different endothelial-specific promoters, Tie2-Cre and VE-cadherin-Cre. These animals have varying levels of diabetes-proneness in their background lineages (Konishi et al., 2017).

The HFD treatment did not interact with the InsR excision to induce any spatial cognitive deficits on the YM or MWM. Post-diet, KO mice showed a greater preference for the novel arm and target quadrant, respectively. Importantly, there were no differences between the KO CHOW and KO HFD groups. However, the KO relative to WT groups were slower to learn the platform location of the MWM during post-diet training. In healthy brain aging, the function of the BBB, the InsR and its signalling cascade are disrupted (Banks et al., 2021; Farrall & Wardlaw, 2009; Hoyer, 2002; Matz & Andriantsitohaina, 2003; Verheggen et al., 2020). Therefore, one possibility is that while our adult male KO mice performed normally during pre-diet training, when tested post-diet (when the age was 10 months old, i.e., middle-aged) there was an interaction between the loss of the BBB InsR and the natural ageing process, exacerbating disruptions to insulin function and contributing to impaired learning on the MWM. Genetic excision of the InsR from neuropeptide-Y (NPY) neurons, abundant in the hippocampus, in middle-aged mice is sufficient to induce cognitive impairments (Goodman et al., 2022). Twelve-month-old mice with the InsR excised from NPY neurons took longer to reach the previous platform location on the final day of the MWM test as compared to wildtype littermates (Goodman et al., 2022). However, obesity also exacerbates age-related BBB disruptions (Tucsek et al., 2014), so it is surprising that there wasn't an interaction between diet and genotype. That is, this deficit in learning was not exclusive to the KO HFD group. This could be linked back to the pre-diet training protection that was possibly offered, particularly if this protection was hippocampal-specific. The testing of younger animals and HFD fed animals without pre-training are required to confirm these explanations though.

4.4. Limitations and future directions

Altogether, the results show that excision of the endothelial InsR left spatial cognition intact. This is in line with pharmacokinetic evidence demonstrating that the endothelial InsR is involved in insulin signalling but not insulin peptide transport (Gray et al., 2017; Hersom et al., 2018; Konishi et al., 2017; Rhea, Rask-Madsen, et al., 2018). Although the PCR validation revealed a trend toward less InsR mRNA in microvessels of KO mice, previous studies have validated the use of this InsR-flox Tie2-Cre genotype (Roudnicky et al., 2017; Vicent et al., 2003), and as such we are confident that the non-significant difference in InsR mRNA expression reflected a lack of power rather than ineffective InsR excision. While the Tie2-Cre transgene used in our experiment is less

endothelial specific than the VE-cadherin-Cre transgene used by others (Konishi et al., 2017; Rhea, Rask-Madsen, et al., 2018), it has not been shown to interfere with other cell types that comprise the BBB, and so we assume the transport mechanisms between the models are equivalent. It is however possible that other BBB cell types expressing the InsR (including neurons, astrocytes, and pericytes) work collectively to regulate InsR function and insulin transport across the BBB (Rhea & Banks, 2019). The significance of cell–cell communication at the BBB and the regulation exerted over it by the CNS remains largely unknown (Rhea & Banks, 2021). Transgenic mouse models lacking the InsR in different cell types, along with pharmacokinetics and *in vitro* culturing, would help tackle these unknowns. For example, injecting fluorescently labeled tracers enables *in vivo* assessment of BBB permeability (Devraj et al., 2018; Hargrave et al., 2016). Employing these assays after InsR excision could inform how loss of the InsR on different cell types modifies BBB insulin transport. Overall, though, coupled with previous evidence (Hersom et al., 2018; Konishi et al., 2017; Rhea, Rask-Madsen, et al., 2018), we are confident our model has demonstrated that there are minimal functional repercussions on spatial cognition after loss of the BBB endothelial InsR.

One caveat in interpreting these conclusions is that only male mice were used in this study as well as in previous *in vivo* pharmacokinetic studies (Konishi et al., 2017; Rhea, Rask-Madsen, et al., 2018). It is broadly accepted that sex differences exist on a range of neurobiological and cognitive measures. For example, genetic profiling of male and female C57BL/6 mice over 15 months revealed different aging trajectories between the sexes (Zhao et al., 2016). Specifically, female brains exhibited earlier onset changes and downregulation of genes involved in insulin and IGF signalling which was not present in age-matched males (Zhao et al., 2016). Similar differences in insulin receptor signalling pathways and responses to centrally administered insulin due to sex, in both rodents and humans, have been repeatedly demonstrated (Benedict et al., 2008; Hallschmid et al., 2008; Hallschmid et al., 2004; Nguyen et al., 2023; Wagner et al., 2022). It is also well established that male and female rodents utilize different spatial strategies during hippocampal-dependent learning tasks (Yagi & Galea, 2019). Importantly, females are at greater risk for developing the hippocampal degeneration and cognitive decline associated with Alzheimer's disease, highlighting the need to understand the unique neurobiology of males and females. Thus, our behavioral and prior pharmacokinetic studies (Konishi et al., 2017; Rhea, Rask-Madsen, et al., 2018) should be replicated in sex-balanced experiments and the current conclusions should not be immediately presumed to apply to females.

If the InsR is not responsible for insulin transport, the question arises as to how then is insulin making its way into the brain? One hypothesis is that a currently unidentified insulin transporter must exist at the BBB (Banks et al., 2022; Pemberton et al., 2022; Rhea, Rask-Madsen, et al., 2018). Indeed, others have begun to explore the unique mechanisms of insulin transcytosis at the BBB (Pemberton et al., 2022). In many cases, the signalling related receptor for a specific peptide is not responsible for its transcytosis across the BBB. For example, ghrelin can cross the BBB regardless of whether its primary signalling receptor is intact or not (Rhea, Salameh, et al., 2018). This idea also fits the assumption that insulin's preferred method of entry into the brain is via the BBB, however some evidence suggests that this mechanism is limited and inefficient (Banks et al., 2012; Kaiyala et al., 2000; Sartorius et al., 2015; Xaio et al., 2001). Alternative theories include that more insulin is being transported into the brain via the CSF than originally thought, that sufficient insulin is produced within the CNS, or, that transport does not rely heavily on active receptor-mediated processes. These ideas have attracted very little attention since their validity was challenged by modelling studies in the 1990s. Yet, novel findings suggest that it is time to revisit them. Several *in vitro* and *in vivo* models have demonstrated the presence of insulin and its precursors throughout multiple regions of the rodent and human brain (see Dakic et al., 2023 for review). For example, in the hippocampus, preproinsulin mRNA, mature insulin, and C-peptide

are expressed (Ghasemi et al., 2013; Mehran et al., 2012) and subpopulations of neurons produce insulin (Kuwabara et al., 2011). While the rate of hippocampal insulin expression is lower than in the pancreas, and the overall biological volumes of *de novo* brain insulin production are unclear, synthesis of enough brain insulin would support the intact spatial capacity that we observed in KO mice, as well as why early modelling studies identified insulin in the CSF (Stein et al., 1983; Woods & Porte, 1977). Regardless, it remains clear from radioactive tracer studies that peripheral insulin can and does enter the brain (Gray et al., 2017; Hersom et al., 2018; Konishi et al., 2017; Rhea, Rask-Madsen, et al., 2018), and thus must somehow navigate barriers, such as the BBB, to gain entry.

4.5. Conclusion

This study is, to our knowledge, the first to comprehensively test the effects of InsR endothelial knockout and HFD on spatial cognition. Our results demonstrate that genetic excision of the InsR from endothelial cells of male mice leaves spatial memory intact. This supports recent findings that blockade or excision of the BBB endothelial InsR interrupts insulin signalling but not transendothelial insulin transport (Gray et al., 2017; Hersom et al., 2018; Konishi et al., 2017; Rhea, Rask-Madsen, et al., 2018). These data represent the first functional evidence that the signalling related InsR is not needed for downstream insulin function in the brain. While the preferred methods of insulin entry into the brain remain unclear, understanding this physiology, and the interactions between insulin resistance, endothelial dysfunction, and cognitive impairments, will provide critical insights into how brain insulin function contributes to the pathogenesis of various cognitive disorders, and how it can be treated.

CRediT authorship contribution statement

J.M. Gladding: Writing – review & editing, Writing – original draft, Visualization, Validation, Methodology, Investigation, Formal analysis, Data curation, Conceptualization. **Z.N. Rafiei:** Writing – review & editing, Investigation. **C.S. Mitchell:** Writing – review & editing, Validation, Resources, Investigation. **D.P. Begg:** Writing – review & editing, Supervision, Methodology, Funding acquisition, Conceptualization.

Data availability

Data will be made available on request.

Acknowledgements

References

Arnold, S. E., Lucki, I., Brookshire, B. R., Carlson, G. C., Browne, C. A., Kazi, H., Bang, S., Choi, B.-R., Chen, Y., McMullen, M. F., & Kim, S. F. (2014). High fat diet produces brain insulin resistance, synaptodendritic abnormalities and altered behavior in mice. *Neurobiology of Disease, 67*, 79–87. https://doi.org/10.1016/j.nbd.2014.03.011

Banks, W. A., Jaspan, J. B., Huang, W., & Kastin, A. J. (1997). Transport of insulin across the blood-brain barrier: Saturability at euglycemic doses of insulin. *Peptides, 18*(9), 1423–1429. https://doi.org/10.1016/S0196-9781(97)00231-3

Banks, W. A., Noonan, C., & Rhea, E. M. (2022). Evidence for an alternative insulin transporter at the blood-brain barrier. *Aging Pathobiol Ther, 4*(4), 100–108. https://doi.org/10.31491/apt.2022.12.100

Banks, W. A., Owen, J. B., & Erickson, M. A. (2012). Insulin in the brain: There and back again. *Pharmacology & Therapeutics, 136*(1), 82–93. https://doi.org/10.1016/j.pharmthera.2012.07.006

Banks, W. A., Reed, M. J., Logsdon, A. F., Rhea, E. M., & Erickson, M. A. (2021). Healthy aging and the blood–brain barrier. *Nature Aging, 1*(3), 243–254. https://doi.org/10.1038/s43587-021-00043-5

Bannerman, D. M., Good, M. A., Butcher, S. P., Ramsay, M., & Morris, R. G. M. (1995). Distinct components of spatial learning revealed by prior training and NMDA receptor blockade. *Nature, 378*(6553), 182–186. https://doi.org/10.1038/378182a0

Baura, G. D., Foster, D. M., Porte, D., Jr, Kahn, S. E., Bergman, R. N., Cobelli, C., & Schwartz, M. W. (1993). Saturable transport of insulin from plasma into the central nervous system of dogs in vivo. A mechanism for regulated insulin delivery to the brain. *Journal of Clinical Investigation, 92*(1), 1824–1830. https://doi.org/10.1172/JCI116773

Benedict, C., Hallschmid, M., Hatke, A., Schultes, B., Fehm, H., Born, J., & Kern, W. (2004). Intranasal insulin improves memory in humans. *Psychoneuroendocrinology, 29*(10), 1326–1334. https://doi.org/10.1016/j.psyneuen.2004.04.003

Benedict, C., Kern, W., Schultes, B., Born, J., & Hallschmid, M. (2008). Differential sensitivity of men and women to anorexigenic and memory-improving effects of intranasal insulin. *The Journal of Clinical Endocrinology & Metabolism, 93*(4), 1339–1344. https://doi.org/10.1210/jc.2007-2606

Benfato, I. D., Quintanilha, A. C. S., Henrique, J. S., Souza, M. A., Rosário, B. d. A., Beserra Filho, J. I. A., Santos, R. L. O., Ribeiro, A. M., Le Sueur Maluf, L., & de Oliveira, C. A. M. (2022). Effects of long-term social isolation on central, behavioural and metabolic parameters in middle-aged mice. *Behavioural Brain Research, 417*, 113630. Doi: Doi: 10.1016/j.bbr.2021.113630.

Boitard, C., Cavaroc, A., Sauvant, J., Aubert, A., Castanon, N., Layé, S., & Ferreira, G. (2014). Impairment of hippocampal-dependent memory induced by juvenile high-fat diet intake is associated with enhanced hippocampal inflammation in rats. *Brain, Behavior, and Immunity, 40*, 9–17. https://doi.org/10.1016/j.bbi.2014.03.005

Boitard, C., Etchamendy, N., Sauvant, J., Aubert, A., Tronel, S., Marighetto, A., Layé, S., & Ferreira, G. (2012). Juvenile, but not adult exposure to high-fat diet impairs relational memory and hippocampal neurogenesis in mice. *22*(11), 2095-2100. Doi: Doi: 10.1002/hipo.22032.

Buie, J. J., Watson, L. S., Smith, C. J., & Sims-Robinson, C. (2019). Obesity-related cognitive impairment: The role of endothelial dysfunction. *Neurobiology of Disease, 132*, Article 104580. https://doi.org/10.1016/j.nbd.2019.104580

Clegg, D., Gotoh, K., Kemp, C., Wortman, M., Benoit, S., Brown, L., D'Alessio, D., Tso, P., Seeley, R., & Woods, S. C. (2011). Consumption of a high-fat diet induces central insulin resistance independent of adiposity. *Physiology & Behavior, 103*(1), 10–16. https://doi.org/10.1016/j.physbeh.2011.01.010

Craft, S., Baker, L. D., Montine, T. J., Minoshima, S., Watson, G. S., Claxton, A., Arbuckle, M., Callaghan, M., Tsai, E., Plymate, S. R., Green, P. S., Leverenz, J., Cross, D., & Gerton, B. (2012). Intranasal insulin therapy for Alzheimer disease and amnestic mild cognitive impairment: A pilot clinical trial. *Archives of Neurology, 69*(1), 29–38. https://doi.org/10.1001/archneurol.2011.233

Dakic, T., Jevdjovic, T., Lakic, I., Ruzicic, A., Jasnic, N., Djurasevic, S., Djordjevic, J., & Vujovic, P. (2023). The expression of insulin in the central nervous system: what have we learned so far? *International Journal of Molecular Sciences, 24*(7). https://doi.org/10.3390/ijms24076586

Dember, W. N., & Fowler, H. (1959). Spontaneous alternation after free and forced trials. *Canadian Journal of Psychology / Revue canadienne de psychologie, 13*(3), 151–154. https://doi.org/10.1037/h0083776

Devraj, K., Guérit, S., Macas, J., & Reiss, Y. (2018). An in vivo blood-brain barrier permeability assay in mice using fluorescently labeled tracers. *Journal of Visualized Experiments, 132*. https://doi.org/10.3791/57038

Farrall, A. J., & Wardlaw, J. M. (2009). Blood–brain barrier: Ageing and microvascular disease – systematic review and meta-analysis. *Neurobiology of Aging, 30*(3), 337–352. https://doi.org/10.1016/j.neurobiolaging.2007.07.015

Foster, W., & Putos, S. (2014). Neglecting the null: The pitfalls of underreporting negative results in preclinical research. *University of Ottawa Journal of Medicine, 4*(1). https://ruor.uottawa.ca/handle/10393/31044.

Ghasemi, R., Haeri, A., Dargahi, L., Mohamed, Z., & Ahmadiani, A. (2013). Insulin in the brain: Sources, localization and functions. *Molecular Neurobiology, 47*(1), 145–171. https://doi.org/10.1007/s12035-012-8339-9

Gladding, J. M., Abbott, K. N., Antoniadis, C. P., Stuart, A., & Begg, D. P. (2018). The effect of intrahippocampal insulin infusion on spatial cognitive function and markers of neuroinflammation in diet-induced obesity. *Frontiers in endocrinology, 9*, 752. https://doi.org/10.3389/fendo.2018.00752

Goncharov, N. V., Nadeev, A. D., Jenkins, R. O., & Avdonin, P. V. (2017). Markers and biomarkers of endothelium: when something is rotten in the state. *Oxidative Medicine and Cellular Longevity, 2017*, 9759735. https://doi.org/10.1155/2017/9759735

Goodman, E. K., Mitchell, C. S., Teo, J., Gladding, J. M., Abbott, K. N., Rafiei, N., Zhang, L., Herzog, H., & Begg, D. P. (2022). The effect of insulin receptor deletion in neuropeptide Y neurons on hippocampal dependent cognitive function in aging mice. *Journal of Integrative Neuroscience, 21*(1). https://doi.org/10.31083/j.jin2101006

Gray, S. M., Aylor, K. W., & Barrett, E. J. (2017). Unravelling the regulation of insulin transport across the brain endothelial cell. *Diabetologia, 60*(8), 1512–1521. https://doi.org/10.1007/s00125-017-4285-4

Haj-ali, V., Mohaddes, G., & Babri, S. (2009). Intracerebroventricular insulin improves spatial learning and memory in male wistar rats. *Behavioural Neuroscience, 123*(6), 1309–1314. https://doi.org/10.1037/a0017722

Hallschmid, M., Benedict, C., Schultes, B., Born, J., & Kern, W. (2008). Obese men respond to cognitive but not to catabolic brain insulin signaling. *International Journal of Obesity, 32*(2), 275–282. https://doi.org/10.1038/sj.ijo.0803722

Hallschmid, M., Benedict, C., Schultes, B., Fehm, H.-L., Born, J., & Kern, W. (2004). Intranasal insulin reduces body fat in men but not in women. *Diabetes, 53*(11), 3024–3029. https://doi.org/10.2337/diabetes.53.11.3024

Hargrave, S., Davidson, T., Zheng, W., & Kinzig, K. (2016). Western diets induce blood-brain barrier leakage and alter spatial strategies in rats. *Behavioral Neuroscience, 130*(1), 123–135. https://doi.org/10.1037/bne0000110

Hays, W. L. (1963). *Statistics for psychologists*. Rinehart and Winston: Holt.

Hersom, M., Helms, H. C., Schmalz, C., Pedersen, T.Å., Buckley, S. T., & Brodin, B. (2018). The insulin receptor is expressed and functional in cultured blood-brain barrier endothelial cells but does not mediate insulin entry from blood to brain. *American Journal of Physiology-Endocrinology and Metabolism, 315*(4), E531–E542. https://doi.org/10.1152/ajpendo.00350.2016

Heyward, F. D., Walton, R. G., Carle, M. S., Coleman, M. A., Garvey, W. T., & Sweatt, J. D. (2012). Adult mice maintained on a high-fat diet exhibit object location memory deficits and reduced hippocampal SIRT1 gene expression. *Neurobiology of Learning and Memory, 98*(1), 25–32. https://doi.org/10.1016/j.nlm.2012.04.005

Hoyer, S. (2002). The aging brain. Changes in the neuronal insulin/insulin receptor signal transduction cascade trigger late-onset sporadic Alzheimer disease (SAD). A mini-review. *Journal of Neural Transmission, 109*(7), 991–1002. https://doi.org/10.1007/s007020200082

Kaiyala, K. J., Prigeon, R. L., Kahn, S. E., Woods, S. C., & Schwartz, M. W. (2000). Obesity induced by a high-fat diet is associated with reduced brain insulin transport in dogs. *Diabetes, 49*(9), 1525–1533. https://doi.org/10.2337/diabetes.49.9.1525

Kern, W., Benedict, C., Schultes, B., Plohr, F., Moser, A., Born, J., Fehm, H. L., & Hallschmid, M. (2006). Low cerebrospinal fluid insulin levels in obese humans. *Diabetologia, 49*(11), 2790–2792. https://doi.org/10.1007/s00125-006-0409-y

Kisanuki, Y. Y., Hammer, R. E., Miyazaki, J.-I., Williams, S. C., Richardson, J. A., & Yanagisawa, M. (2001). Tie2-cre transgenic mice: A new model for endothelial cell-lineage analysis in vivo. *Developmental Biology, 230*(2), 230–242. https://doi.org/10.1006/dbio.2000.0106

Kondo, T., Vicent, D., Suzuma, K., Yanagisawa, M., King, G. L., Holzenberger, M., & Kahn, C. R. (2003). Knockout of insulin and IGF-1 receptors on vascular endothelial cells protects against retinal neovascularization. *The Journal of clinical investigation, 111*(12), 1835–1842. https://doi.org/10.1172/JCI17455

Konishi, M., Sakaguchi, M., Lockhart, S. M., Cai, W., Li, M. E., Homan, E. P., Rask-Madsen, C., & Kahn, C. R. (2017). Endothelial insulin receptors differentially control insulin signaling kinetics in peripheral tissues and brain of mice. *Proceedings of the National Academy of Sciences, 114*(40), E8478–E8487. https://doi.org/10.1073/pnas.1710625114

Kraeuter, A.-K., Guest, P. C., & Sarnyai, Z. (2019). The Y-Maze for Assessment of Spatial Working and Reference Memory in Mice. In P. C. Guest (Ed.), *Pre-Clinical Models: Techniques and Protocols* (pp. 105-111). Springer New York. Doi: 10.1007/978-1-4939-8994-2_10.

Kuboki, K., Jiang Zhen, Y., Takahara, N., Ha Sung, W., Igarashi, M., Yamauchi, T., Feener Edward, P., Herbert Terrance, P., Rhodes Christopher, J., & King George, L. (2000). Regulation of endothelial constitutive nitric oxide synthase gene expression in endothelial cells and in vivo. *Circulation, 101*(6), 676–681. https://doi.org/10.1161/01.CIR.101.6.676

Kuwabara, T., Kagalwala, M. N., Onuma, Y., Ito, Y., Warashina, M., Terashima, K., Sanosaka, T., Nakashima, K., Gage, F. H., & Asashima, M. (2011). Insulin biosynthesis in neuronal progenitors derived from adult hippocampus and the olfactory bulb. *EMBO Molecular Medicine, 3*(12), 742–754. https://doi.org/10.1002/emmm.201100177

Lee, Y.-K., Uchida, H., Smith, H., Ito, A., & Sanchez, T. (2019). The isolation and molecular characterization of cerebral microvessels. *Nature Protocols, 14*(11), 3059–3081. https://doi.org/10.1038/s41596-019-0212-0

Leyh, J., Winter, K., Reinicke, M., Ceglarek, U., Bechmann, I., & Landmann, J. (2021). Long-term diet-induced obesity does not lead to learning and memory impairment in adult mice. *PloS one, 16*(9), e0257921.

Matz, R. L., & Andriantsitohaina, R. (2003). Age-related endothelial dysfunction. *Drugs & Aging, 20*(7), 527–550. https://doi.org/10.2165/00002512-200320070-00005

McNay, E. C., Ong, C., McCrimmon, R., Cresswell, J., Bogan, J., & Sherwin, R. (2010). Hippocampal memory processes are modulated by insulin and high-fat-induced insulin resistance. *Neurobiological Learning Memory, 93*(4), 546–553. https://doi.org/10.1016/j.nlm.2010.02.002

Mehran, A. E., Templeman, N. M., Brigidi, G. S., Lim, G. E., Chu, K.-Y., Hu, X., Botezelli, J. D., Asadi, A., Hoffman, B. G., Kieffer, T. J., Bamji, S. X., Clee, S. M., & Johnson, J. D. (2012). Hyperinsulinemia drives diet-induced obesity independently of brain insulin production. *Cell Metabolism, 16*(6), 723–737. https://doi.org/10.1016/j.cmet.2012.10.019

Meijer, R. I., Gray, S. M., Aylor, K. W., & Barrett, E. J. (2016). Pathways for insulin access to the brain: The role of the microvascular endothelial cell. *American Journal of Physiology-Heart and Circulatory Physiology, 311*(5), H1132–H1138. https://doi.org/10.1152/ajpheart.00081.2016

Moosavi, M., Naghdi, N., Maghsoudi, N., & Zahedi Asl, S. (2006). The effect of intrahippocampal insulin microinjection on spatial learning and memory. *Hormones and Behavior, 50*(5), 748–752. https://doi.org/10.1016/j.yhbeh.2006.06.025

Morris, R. G. M. (1981). Spatial localization does not require the presence of local cues. *Learning and Motivation, 12*(2), 239–260. https://doi.org/10.1016/0023-9690(81)90020-5

Nguyen, V., Thomas, P., Pemberton, S., Babin, A., Noonan, C., Weaver, R., Banks, W. A., & Rhea, E. M. (2023). Central nervous system insulin signaling can influence the rate of insulin influx into brain. *Fluids and Barriers of the CNS, 20*(1), 28. https://doi.org/10.1186/s12987-023-00431-6

Pemberton, S., Galindo, D. C., Schwartz, M. W., Banks, W. A., & Rhea, E. M. (2022). Endocytosis of insulin at the blood-brain barrier [Original Research]. *Frontiers in Drug Delivery, 2.* https://doi.org/10.3389/fddev.2022.1062366

Pratchayasakul, W., Kerdphoo, S., Petsophonsakul, P., Pongchaidecha, A., Chattipakorn, N., & Chattipakorn, S. C. (2011). Effects of high-fat diet on insulin receptor function in rat hippocampus and the level of neuronal corticosterone. *Life Sciences, 88*(13–14), 619–627. https://doi.org/10.1016/j.lfs.2011.02.003

Reger, M. A., Watson, G. S., Green, P. S., Wilkinson, C. W., Baker, L. D., Cholerton, B., Fishel, M. A., Plymate, S. R., Breitner, J. C. S., DeGroodt, W., Mehta, P., & Craft, S. (2008). Intranasal insulin improves cognition and modulates [beta]-amyloid in early AD [Research Article]. *Neurology, 70*(6), 440–448. https://doi.org/10.1212/01.WNL.0000265401.62434.36

Rhea, E. M., & Banks, W. A. (2019). Role of the blood-brain barrier in central nervous system insulin resistance. *Frontiers in neuroscience, 13*, 521. https://doi.org/10.3389/fnins.2019.00521

Rhea, E. M., & Banks, W. A. (2021). A historical perspective on the interactions of insulin at the blood-brain barrier. *Journal of Neuroendocrinology, 33*(4), e12929.

Rhea, E. M., Rask-Madsen, C., & Banks, W. A. (2018). Insulin transport across the blood–brain barrier can occur independently of the insulin receptor. *The Journal of Physiology, 596*(19), 4753–4765. https://doi.org/10.1113/JP276149

Rhea, E. M., Salameh, T. S., Gray, S., Niu, J., Banks, W. A., & Tong, J. (2018). Ghrelin transport across the blood-brain barrier can occur independently of the growth hormone secretagogue receptor. *Molecular Metabolism, 18*, 88–96. https://doi.org/10.1016/j.molmet.2018.09.007

Rivera-Irizarry, J. K., Skelly, M. J., & Pleil, K. E. (2020). Social isolation stress in adolescence, but not adulthood, produces hypersocial behavior in adult male and female C57BL/6J mice [original research]. *Frontiers in Behavioral Neuroscience, 14.* https://doi.org/10.3389/fnbeh.2020.00129

Roudnicky, F., Dieterich, L. C., Poyet, C., Buser, L., Wild, P., Tang, D., Camenzind, P., Ho, C. H., Otto, V. I., & Detmar, M. (2017). High expression of insulin receptor on tumour-associated blood vessels in invasive bladder cancer predicts poor overall and progression-free survival. *The Journal of Pathology, 242*(2), 193–205. https://doi.org/10.1002/path.4892

Sanders, M. J., & Fanselow, M. S. (2003). Pre-training prevents context fear conditioning deficits produced by hippocampal NMDA receptor blockade. *Neurobiology of Learning and Memory, 80*(2), 123–129. https://doi.org/10.1016/S1074-7427(03)00040-6

Sartorius, T., Peter, A., Heni, M., Maetzler, W., Fritsche, A., Häring, H.-U., & Hennige, A. M. (2015). The brain response to peripheral insulin declines with age: A contribution of the blood-brain barrier? *PloS one, 10*(5), e0126804.

Schwartz, M. W., Bergman, R. N., Kahn, S. E., Taborsky, G. J., Fisher, L. D., Sipols, A. J., Woods, S. C., Steil, G. M., & Porte, D., Jr (1991). Evidence for entry of plasma insulin into cerebrospinal fluid through an intermediate compartment in dogs. Quantitative aspects and implications for transport. *Journal of Clinical Investigation, 88*(4), 1272–1281. https://doi.org/10.1172/JCI115431

Spence, K. W., & Lippitt, R. (1946). An experimental test of the sign-gestalt theory of trial and error learning. *Journal of Experimental Psychology, 36*(6), 491–502. https://doi.org/10.1037/h0062419

Stein, L. J., Dorsa, D. M., Baskin, D. G., Figlewicz, D. P., Ikeda, H., Frarikmann, S. P., Greenwood, M. R. C., Porte, D., Jr, & Woods, S. C. (1983). Immunoreactive insulin levels are elevated in the cerebrospinal fliud of genetically obese zucker rats. *Endocrinology, 113*(6), 2299–2301. https://doi.org/10.1210/endo-113-6-2299 %J Endocrinology

Tran, D. M. D., & Westbrook, R. F. (2017). A high-fat high-sugar diet-induced impairment in place-recognition memory is reversible and training-dependent. *Appetite, 110*, 61–71. https://doi.org/10.1016/j.appet.2016.12.010

Tucsek, Z., Toth, P., Sosnowska, D., Gautam, T., Mitschelen, M., Koller, A., Szalai, G., Sonntag, W. E., Ungvari, Z., & Csiszar, A. (2014). Obesity in aging exacerbates blood-brain barrier disruption, neuroinflammation, and oxidative stress in the mouse hippocampus: Effects on expression of genes involved in beta-amyloid generation and Alzheimer's disease. *The Journals of Gerontology. Series A, Biological Sciences and Medical Sciences, 69*(10), 1212–1226. https://doi.org/10.1093/gerona/glt177

Valladolid-Acebes, I., Stucchi, P., Cano, V., Fernández-Alfonso, M. S., Merino, B., Gil-Ortega, M., Fole, A., Morales, L., Ruiz-Gayo, M., & Olmo, N. D. (2011). High-fat diets impair spatial learning in the radial-arm maze in mice. *Neurobiology of Learning and Memory, 95*(1), 80–85. https://doi.org/10.1016/j.nlm.2010.11.007

Verheggen, I. C. M., de Jong, J. J. A., van Boxtel, M. P. J., Postma, A. A., Jansen, J. F. A., Verhey, F. R. J., & Backes, W. H. (2020). Imaging the role of blood–brain barrier disruption in normal cognitive ageing. *GeroScience, 42*(6), 1751–1764. https://doi.org/10.1007/s11357-020-00282-1

Vicent, D., Ilany, J., Kondo, T., Naruse, K., Fisher, S. J., Kisanuki, Y. Y., Bursell, S., Yanagisawa, M., King, G. L., & Kahn, C. R. (2003). The role of endothelial insulin signaling in the regulation of vascular tone and insulin resistance. *The Journal of Clinical Investigation, 111*(9), 1373–1380. https://doi.org/10.1172/JCI15211

Wagner, L., Veit, R., Fritsche, L., Häring, H.-U., Fritsche, A., Birkenfeld, A. L., Heni, M., Preissl, H., & Kullmann, S. (2022). Sex differences in central insulin action: Effect of intranasal insulin on neural food cue reactivity in adults with normal weight and overweight. *International Journal of Obesity, 46*(9), 1662–1670. https://doi.org/10.1038/s41366-022-01167-3

Williams, I. L., Wheatcroft, S. B., Shah, A. M., & Kearney, M. T. (2002). Obesity, atherosclerosis and the vascular endothelium: Mechanisms of reduced nitric oxide bioavailability in obese humans. *International Journal of Obesity, 26*(6), 754–764. https://doi.org/10.1038/sj.ijo.0801995

Woods, S. C., & Porte, D., Jr (1977). Relationship between plasma and cerebrospinal fluid insulin levels of dogs. *American Journal of Physiology, 233*(4), E331. https://doi.org/10.1152/ajpendo.1977.233.4.E331

Xaio, H., Banks, W. A., Niehoff, M. L., & Morley, J. E. (2001). Effect of LPS on the permeability of the blood–brain barrier to insulin. *Brain Research, 896*(1), 36–42. https://doi.org/10.1016/S0006-8993(00)03247-9

Yagi, S., & Galea, L. (2019). Sex differences in hippocampal cognition and neurogenesis. *Neuropsychopharmacology Reviews, 44*, 200–213. https://doi.org/10.1038/s41386-018-0208-4

Zhao, L., Mao, Z., Woody, S., & Brinton, R. (2016). Sex differences in metabolic aging of the brain: Insights into female susceptibility to Alzheimer's disease. *Neurobiology of Aging, 42*. https://doi.org/10.1016/j.neurobiolaging.2016.02.011

Zhao, W., Chen, H., Xu, H., Moore, E., Meiri, N., Quon, M. J., & Alkon, D. L. (1999). Brain Insulin Receptors and Spatial Memory: Correlated changes in gene expression, tyrosine phosphorylation, and signaling molecules in the hippocampus of water maze trained rats. *Journal of Biological Chemistry, 274*(49), 34893–34902. https://doi.org/10.1074/jbc.274.49.34893